An aqueous chemistry module for a three-dimensional cloud resolving model: sulfate redistribution

DRAGANA VUJOVIĆ* and VLADAN VUČKOVIĆ**

University of Belgrade, Faculty of Physics, Department of Meteorology, Dobračina 16, Belgrade, Serbia

Abstract: An aqueous chemistry module was created and included into a complex 3D cloud-resolving mesoscale advanced regional prediction system (ARPS) model to examine the characteristics of in-cloud sulfate. The complex orography of Serbia was included in the model. The chemical species included in the module were sulfur dioxide, sulfate ion, ammonium ion, hydrogen peroxide and ozone. Six water categories are considered: water vapor, cloud water, rain, cloud ice, snow and hail. Each chemical species in each microphysical category was represented by a differential equation of mass continuity. This paper gives a detailed description of the chemistry module and demonstrates the utility of an atmospheric model coupled with the chemistry module in forecasting the redistribution of chemical species in all water categories. The main mean microphysical and chemical conversion rates of sulfate averaged over a 2 h simulation period for a base run were for the oxidation of S(IV) in rain water and cloud water, SO_4^{2-} scavenging by Brownian diffusion in cloud droplets and cloud ice as well as the impact scavenging of SO_4^{2-} by rain. The calculated values of sulfates in all water categories and the shape of the sulfate profiles depend on radar reflectivity.

Keywords: oxidation; sulfate transfer; cumulonimbus; microphysics; mass transfer.

INTRODUCTION

Clouds play an important role in environmental redistribution of chemistry species. The average global cloud coverage over the oceans is estimated at 65 % and over land at 52 %,[1] so it is clear that clouds play the role of a "large factory" for the aqueous-phase production of chemistry species. The clouds receive trace gases from their inflow regions, their wind redistributes the gases and the clouds transform the gases through gas and aqueous-phase chemistry. The most important gas that leads to acidification is sulfur dioxide. When clouds are present, the

loss rate of atmospheric SO_2 is faster than can be explained by gas phase chemistry alone. This rate of loss is due to reactions in the liquid water droplets where acids are produced. Acid rain can have harmful effects on the environment and on human health through the process of wet deposition.

The first atmospheric models had simple dynamics and microphysics,[2] but in time, the models become more complex. Taylor[3] used a 1.5-dimensional Eulerian cumulus cloud model to examine the characteristics of the in-cloud chemistry. Studies by Tremblay and Leighton[4] and Niewiadomski[5] used three-dimensional cloud chemistry models, but they focused on warm convective clouds only. Scamarock et al.[6] examined tracer transport in 3D simulations, but only on flat ground. Yin et al.[7] examined trace gas redistribution using a two-dimensional cloud model with detailed microphysics and spectral treatment of gas scavenging. Barth et al.[8] examined the redistribution of trace gases during deep convection. Spiridonov and Ćurić[9] examined the relative importance of scavenging, oxidation and ice-phase chemistry in sulfate production in 2D and 3D model runs. This study takes a step forward by developing a new chemistry module and coupling it with a very comprehensive 3D mesoscale atmospheric model. The real orography is included in the model. This paper describes detailed chemistry parameterization. The aim was to demonstrate the fact that a relatively simple chemical module coupled with a comprehensive cloud-resolving model with detailed microphysics could be used as a diagnostic and prognostic tool for chemical species.

EXPERIMENTAL

Description of atmospheric numerical model

A very comprehensive 3D cloud-resolving mesoscale advanced regional prediction system (ARPS) model developed in the Center for Analysis and Prediction of Storms (CAPS) at the University of Oklahoma[10,11] was used to simulate a Cumulonimbus (Cb) life cycle in conditions of a real orography.[12,13]. This model numerically integrates time-dependent, non-hydrostatic and fully compressible equations. The model uses the Lin[14] bulk-water microphysical scheme and represents six water categories: water vapor, cloud water, cloud ice, rain, snow, hail. Rain, hail and snow are each represented by the Marshall–Palmer distribution.[15] Cloud droplets and non-precipitating cloud ice are supposed to be monodispersing. Turbulence was treated by 1.5 order turbulent kinetic energy formulation. The advection of momentum and scalars were treated with a 4th-order scheme in the horizontal direction and 2nd-order scheme in the vertical direction. Radiating (open) conditions were used for lateral boundaries. Rigid-wall boundary conditions were applied for the top and on the bottom of the domain. The large time step was 6 s and the small step (for acoustic waves) was 1 s.

Description of the chemistry module

This section contains the development of the equations that were used to describe the chemical species incorporated in the cloud model. The chemical module is based on the sulfate chemistry taken from Rutledge et al.,[16] Taylor,[3] and Spiridonov and Ćurić.[17] Five chemical species are carried explicitly into the model: SO_2, O_3, H_2O_2, SO_4^{2-} and NH_4^+ in the

form of mixing ratios. All chemical reactions included in the module with the appropriate coefficients are given in Table I.

TABLE I. Equilibrium reactions and rate constants. The equilibrium constants are of the form $k = k_{298} \times \exp(-\Delta H_{298}/R(1/298-1/T))$, where T is the temperature, K[18]

Reaction	k_{298} / mol dm^{-3} s^{-1}	$(-\Delta H_{298}/R)$ / K
$SO_2(g) \leftrightarrows SO_2(aq)$	1.23	3120
$SO_2(aq) \leftrightarrows HSO_3^- + H^+$	1.3×10^{-2}	−2000
$HSO_3^- \leftrightarrows SO_3^{2-} + H^+$	6.3×10^{-8}	−1495
$O_3(g) \leftrightarrows O_3(aq)$	1.15×10^{-2}	−2560
$H_2O_2(g) \leftrightarrows H_2O_2(aq)$	8.33×10^4	−7379
$H_2O_2(aq) \leftrightarrows HO_2^- + H^+$	2.2×10^{-12}	3700
$NH_3(g) \leftrightarrows NH_3(aq)$	92,7	−4085
$S(IV) + H_2O_2 \rightarrow S(VI) + H_2O$	7.5×10^7	4750

The model was formulated in terms of Continuity equations:

$$\frac{\partial q_{i,j}}{\partial t} + \mathbf{V} \cdot \nabla q_{i,j} - FR_{i,j} = S_{i,j} + CH_{i,j} \qquad (1)$$

where $q_{i,j}$ is the mixing ratio of chemical species i in the water category j (e.g., $q_{SO_4,c}$ denotes the cloud water SO_4^{2-} mixing ratio, $q_{SO_4,i}$ denotes the cloud ice SO_4^{2-} mixing ratio), $\mathbf{V} \cdot \nabla q_{i,j}$ is the advection of the chemical species i in water category j by the wind $\mathbf{V} = (u, v, w)$, $FR_{i,j}$ denotes the terminal velocity for hydrometeors, $S_{i,j}$ are the subgrid contribution terms (mixing, turbulence) and $CH_{i,j}$ are the source or sink chemical transformation terms that represent either the transfer of the chemical species from one microphysical category to another (e.g., cloud water sulfate to cloud ice sulfate by riming) or a chemical reaction (e.g., oxidation of cloud water SO_2 to cloud water sulfate). Two assumptions were used:[3,16]

a) over the relatively short time scales that characterize cloud interactions, aqueous phase chemistry is dominant. Therefore, gas phase chemistry was neglected.

b) Aqueous-phase photochemistry contributes only in the secondary sense to the scavenging of sulfur and nitrogen species in clouds, and can therefore be neglected.

The mass transfer between gas and liquid phases

The Henry Law equilibrium does not always exist between water drops and the air.[19] In this study, the Henry Law and a more detailed mass transfer approach that does not assume gas–liquid equilibrium were used. The rate of mass transport between gas species i and a group of aqueous drops with radius r and number concentration of N_r (per mole of air), can be written as:[20]

$$\frac{dM_{i,r}}{dt} = \frac{3\eta D_{g,i} N_{Sh,i}}{R^* T r} \left(V_r N_r p_i - \frac{M_{i,r}}{K^*_{H,i}} \right), \qquad (2)$$

where $M_{i,r}$ is the molar mixing ratio (with respect to air) of gas species i inside drops with radius r; $D_{g,i}$ the diffusivity of gas species i in the air; $N_{Sh,i}$ the Sherwood number; p_i the partial pressure of gas species i in the environment; $K^*_{H,i}$ the effective Henry Law coefficient of species i, R^* the universal gas constant; T the temperature and η a factor to account for the free-molecular effect on the mass transfer rate.[21] Based on previous studies,[17,20,22] a value of $\eta = 0.1$ was used in the simulations for all the species. The effective Henry Law coefficient,

$K^*_{\text{H},i}$, for a species i that undergoes aqueous phase dissociation differs from the Henry Law coefficient $K_{\text{H},i}$ for a molecule, as it accounts for the ionic forms of the dissolved gas.[23]

As dissolved gasses do not normally contribute to the drop size, Eq. (2) becomes a linear first order differential equation that can be solved analytically as:

$$M_{i,\text{r}}(t+\Delta t) = A(t) + [M_{i,\text{r}}(t) - A(t)]\exp(B\Delta t) \qquad (3)$$

where t is the time step for gas dissolution and A and B are:

$$A(t) = \frac{4}{3}\pi r^2 N_\text{r} p_i(t) K^*_{\text{H},i}; \; B = -\frac{3D_{\text{g},i} N_{\text{Sh},i}\, \eta}{r^2 R^* T K^*_{\text{H},i}} \; . \qquad (4)$$

Sulfate chemistry parameterization terms

Sulfur dioxide is the dominant anthropogenic pollutant in air that contains sulfur. Its presence in the troposphere of the Northern Hemisphere is the result of direct anthropogenic emissions, *i.e.,* combustion of fossil fuels. SO_2 is effectively removed from the atmosphere through processes of dry and moist deposition. However, the dominant mechanism for removing SO_2 from the atmosphere is oxidation, either in the gaseous or liquid phase. The creation of sulfates through the oxidation of SO_2 is an important process with changing aerosol radiation effects. A schematic representation of all the chemical and microphysical processes for SO_2 and SO_4^{2-} that are parameterized in the chemical module is presented in Fig. 1. The left side of Fig. 1 is related to SO_2 and its transport from air to cloud droplets and rain drops (calculated using the exact kinetic mass transport approach), as well as its oxidation in cloud droplets and rain drops by ozone and hydrogen peroxide, whereby sulfate is formed. The rest of the graph shows microphysical processes that transport sulfate from one water category to another.

Ammonium source terms

Ammonium is neither created nor destroyed in the chemical reactions modeled here. Here, it is assumed that the sulfate aerosol is composed of ammonium bisulfate $(NH_4)_2SO_4$. Therefore, ammonium is treated like sulfate. The terms *PS*3–*PS*8, *PS*11–*PS*25 (calculation details are given in Supplementary material) represent the source-sink terms for ammonium (*PN*1–*PN*13, *PN*15–*PN*22), but the mixing ratios for SO_4^{2-} should be replaced by the mixing ratios for NH_4^+. The nucleation scavenging efficiency for ammonium is assumed the same as the nucleation scavenging efficiency for sulfate.

Hydrogen peroxide, ozone and S(IV) source-sink terms

The source-sink terms for H_2O_2 and O_3 include an equilibration between gas and aqueous phases, kinetic mass transport, reduction due to the oxidation of S(IV) in cloud droplets and rain, and a set of microphysical transfer and conversions among the different water categories. As this is a short paper, details of the sources and sinks terms for H_2O_2, O_3 and S(IV) will not be given herein.

Model initialization

A single summer sounding, providing profiles of temperature, humidity, speed and direction of wind, initializes the use of a complex atmospheric model coupled with the chemistry module. The real orography of the Serbian region is used as a very important factor in cumulonimbus formation. The centre of the domain is at 43.8° N, 20° E. It represents the Zapadna Morava Valley (mean height above sea level 300 m), and its surrounding environment. Space resolution in the model is 1000 m in the horizontal and 500 m in the vertical direction.

The domain size is 112 km×112 km×16 km. A two-hour forecast is made. It is assumed that initial concentrations of the chemical fields fall off exponentially from the given values of mixing ratios at the lowest model level[3] for a continental background (CB) and for a polluted background (PB).
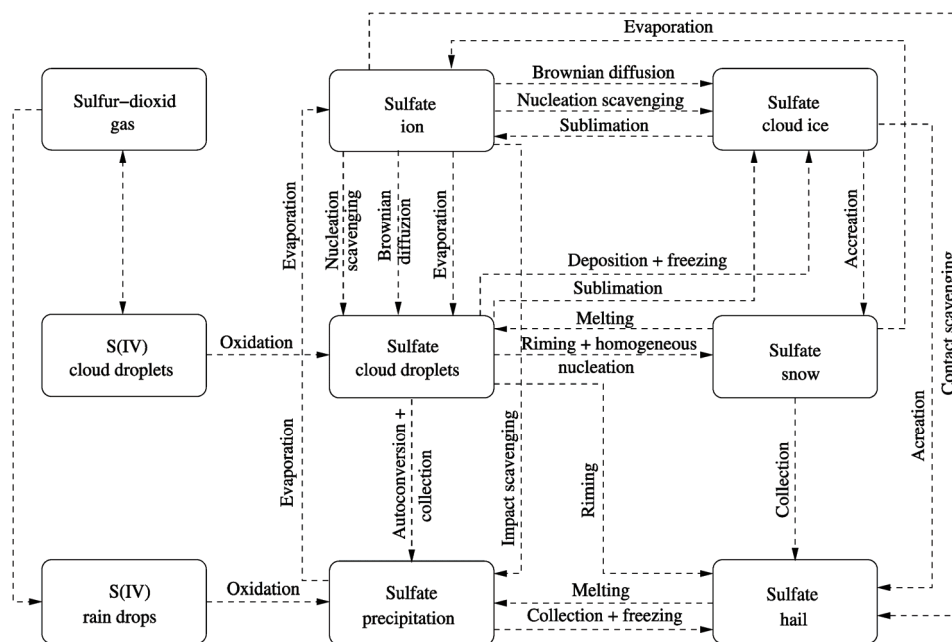

Fig. 1. Scheme of sulfur dioxide (SO_2) and sulfate (SO_4^{2-}) reactions.

RESULTS AND DISCUSSION

Several numerical experiments were designed to verify the developed method of using a chemistry module coupled with a 3D atmospheric model. In the base run (fully kinetic calculation of gas dissolution into cloud droplets and rain drops, calculation of nucleation and impact scavenging of aerosols, S(IV) oxidation by O_3 and H_2O_2 in cloud and rain water, ice phase simulation, orography included), the integrated sulfur mass removed by wet deposition was 22.3 kg for CB, and 60.0 kg for PB, which is in agreement with the results of Spiridonov and Ćurić.[9] The total mass of NH_4^+ incorporated in the precipitation was 8.03 kg for PB and 1.55 kg for CB, which is in agreement with the results of Taylor,[3] i.e., 10.5 kg for PB and 2.03 kg for CB. If the oxidation was neglected, the integrated sulfur mass removed by wet deposition was 16.5 (CB) and 32.1 % (PB) of sulfur mass in the base run. Spiridonov and Ćurić[9] obtained values of 24.1 (CB) and 25.7 % (PB). This difference arises from the different parameterization of oxidetion. The omission of scavenging processes gives 82.9 (CB) and 67.8 % (PB) of the total sulfur deposited in the base run (64.6 (CB) and 68.8 % (PB) in Spirido-

nov and Ćurić[9]). Ignoring the ice phase in the chemistry results in an increase by a factor of 1.5 in the sulfur mass deposited for CB (149.6 %), which is in accordance with the conclusion of Taylor[3] (tests of the ice phase impact on in-cloud chemistry and deposition indicated that the total sulfur mass deposited was increased by about a factor of two relative to the base run case). According to Molder et al.,[26] including ice phase processes in dynamics modeling leads to lower values of sulfate in the liquid phase when convection is present. Regarding the meteorological part of the model, there was agreement between the calculated and observed radar reflectivity.[12] These results correspond with the published results of other authors; thus, the developed model can be considered valid.

The integration (base run) includes mass transport calculations from gas to liquid phase, oxidation of S(IV) by O_3 and H_2O_2, nucleation and impact scavenging and ice phase simulation. In the 10th minute of integration, a cloud was formed. The cloud developed on the mountaintop and then moved along the Zapadna Morava Valley. The cumulative mass of the sulfate, i.e., the sum of the mass of sulfate in gas phase, cloud water, rainwater, cloud ice, snow and hail in every step is shown in Fig. 2. As it is a source for sulfate in other water categories, the mass of sulfate in the gas phase gradually decreased from the initial va-
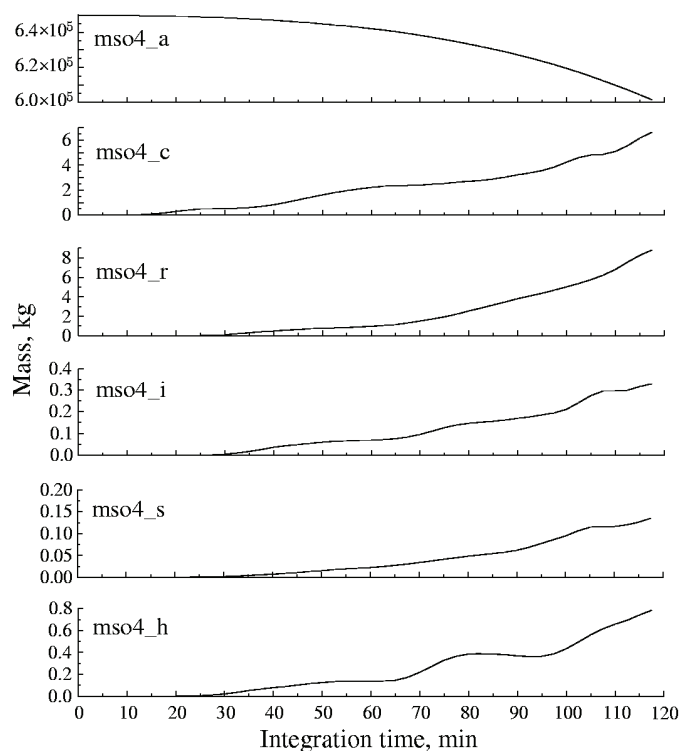

Fig. 2. The cumulative mass of sulfate.

lues. As cloud water formed during the integration, sulfates appear in cloud water at the 10th minute and from the 30th minute in rainwater, snow, hail and cloud ice.

The main mean microphysical and chemical conversion rates of sulfate averaged over a 2-h simulation period for the base run were for the oxidation of S(IV) in rain water and cloud water $PS9 = 4.61{\times}10^{-11}$, $PS9hp = 2.79{\times}10^{-12}$, $PS2 == 2.89{\times}10^{-13}$), SO_2^{4-} scavenging by Brownian diffusion in cloud droplets and cloud ice $PS4cw = 4.91{\times}10^{-11}$ and $PS4ci = 7.82{\times}10^{-12}$, the impact scavenging of SO_2^{4-} by rain $PS6 = 2.08{\times}10^{-11}$, autoconversion of cloud water to form rain, accretion of cloud water by rain, accretion of cloud water by snow $PS11 = = 4.43{\times}10^{-12}$, and the transfer of SO_2^{4-} from cloud ice to snow as a result of autoconversion of cloud ice to form snow, the accretion of cloud ice by snow and the accretion of cloud ice by rain $PS25 = 1.21{\times}10^{-12}$). The calculated radar reflectivity (CRR), which is a good indicator of cloud development, is presented in Fig. 3. The figure shows the horizontal plane on the surface in the 85th minute of integration. At this moment, the cloud is in a mature stage of development, with three "separated" cells with a large CRR: point A (59, 73 km), B (70, 85 km) and C (75, 60 km). The CRR at points A and C was approximately 50 dBz, and at point B nearly 55 dBz.
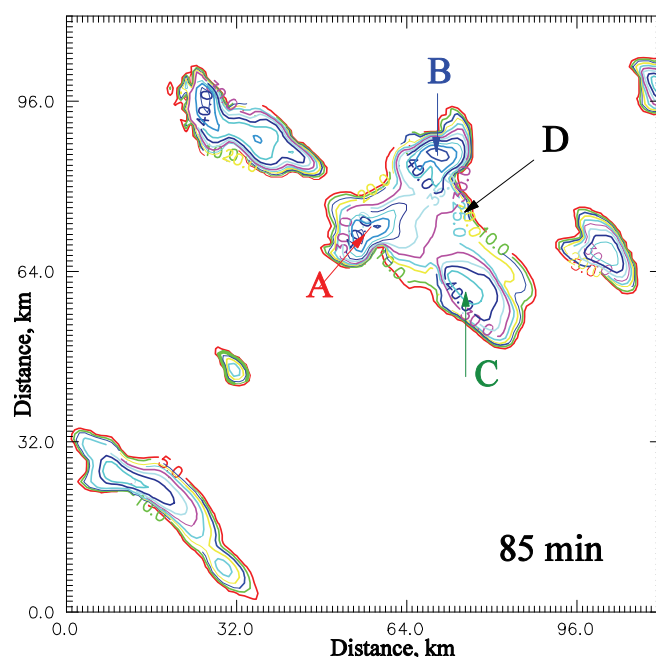

Fig. 3. The radar reflectivity, dBz, in the (x, y) plane on the surface in the 85th minute of integration. The three cells with maximum reflectivity have the coordinates: A (58, 73 km), B (70, 85 km) and C (75, 60 km). Point D (75, 75 km) is at periphery of the cloud.

The vertical profiles of the sulfate following cumulonimbus trajectory could provide considerable information about sulfate redistribution in the troposphere. The vertical profiles of SO_4^{2-} in all categories of water at points A, B and C are shown in Figs. 4–6, respectively. The maximum value of $q_{SO_4^{2-},c}$ in the layer of air above point A was at a height of 5 km and its value was 0.80 µg kg^{-1}, $q_{SO_4^{2-},r}$
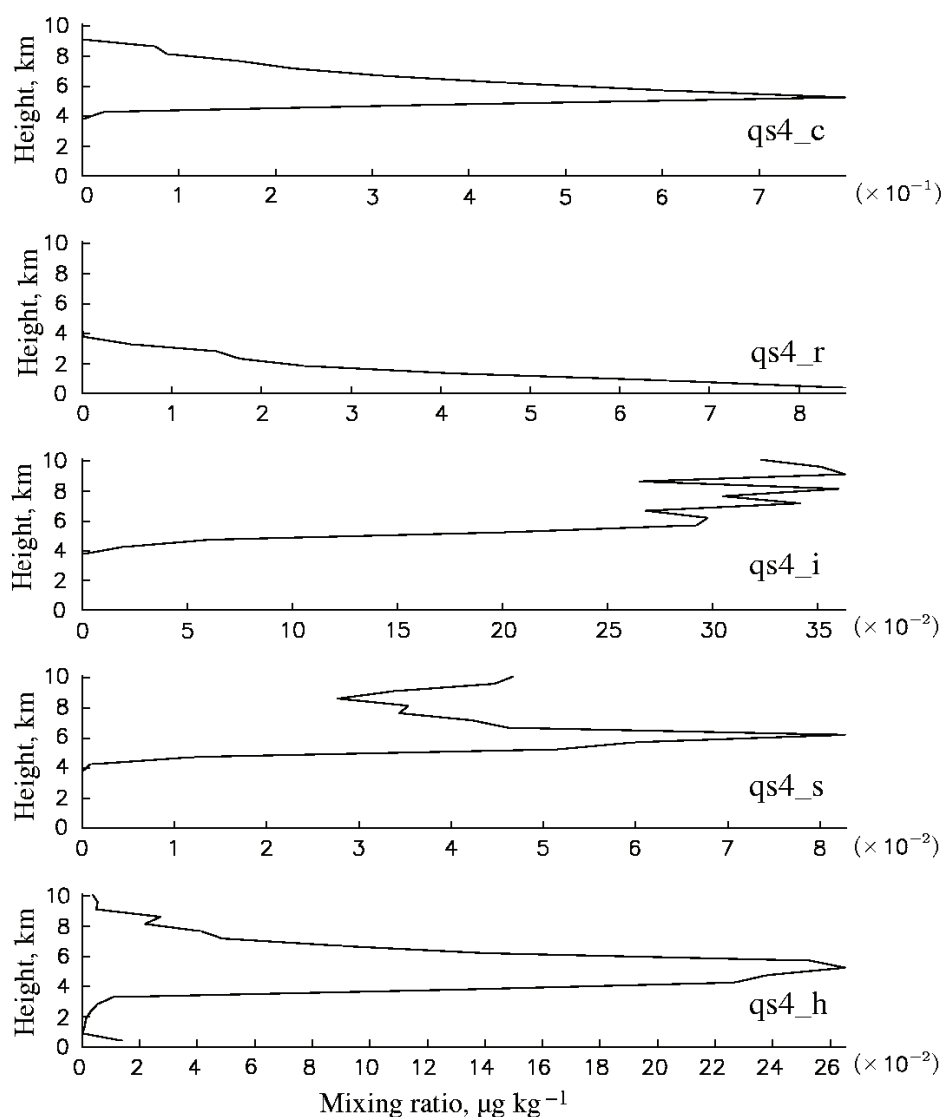

Fig. 4. The vertical profiles of the SO_4^{2-} mixing ratio, µg kg^{-1}, in different water categories: in cloud water ($q_{s4,c}$), rain ($q_{s4,r}$), cloud ice ($q_{s4,i}$), snow ($q_{s4,s}$) and hail ($q_{s4,h}$) for the cell A (58, 73 km).

at the surface was 9.0 µg kg^{-1}, $q_{SO_4^{2-},i}$ at a height of nearly 9 km was 0.35 µg kg^{-1}, $q_{SO_4^{2-},s}$ at a height of about 6 km was 0.08 µg kg^{-1}, and $q_{SO_4^{2-},h}$ at a height of 5.5 km was 0.26 µg kg^{-1}. The profiles above the other two vorticities (B and C) could be analyzed similarly. The shapes of the profiles were similar and had similar values of the sulfate mixing ratios.
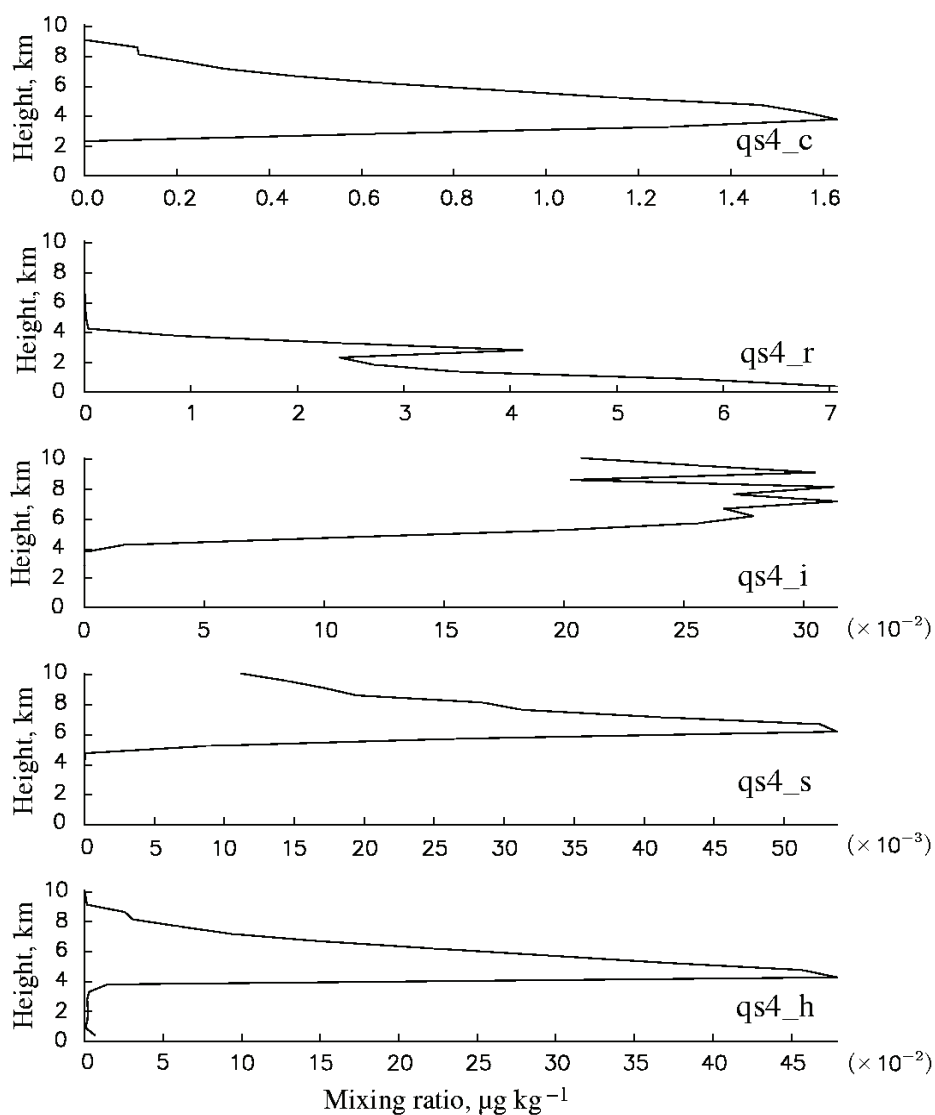

Fig. 5. The vertical profiles of the SO$_4^{2-}$ mixing ratio, µg kg^{-1}, in different water categories: in cloud water ($q_{s4,c}$), rain ($q_{s4,r}$), cloud ice ($q_{s4,i}$), snow ($q_{s4,s}$) and hail ($q_{s4,h}$) for the cell B (70, 85 km).

Fig. 6. The vertical profiles of the SO_4^{2-} mixing ratio, μg kg^{-1}, in different water categories: in cloud water ($q_{s4,c}$), rain ($q_{s4,r}$), cloud ice ($q_{s4,i}$), snow ($q_{s4,s}$) and hail ($q_{s4,h}$) for the cell C (75, 60 km).

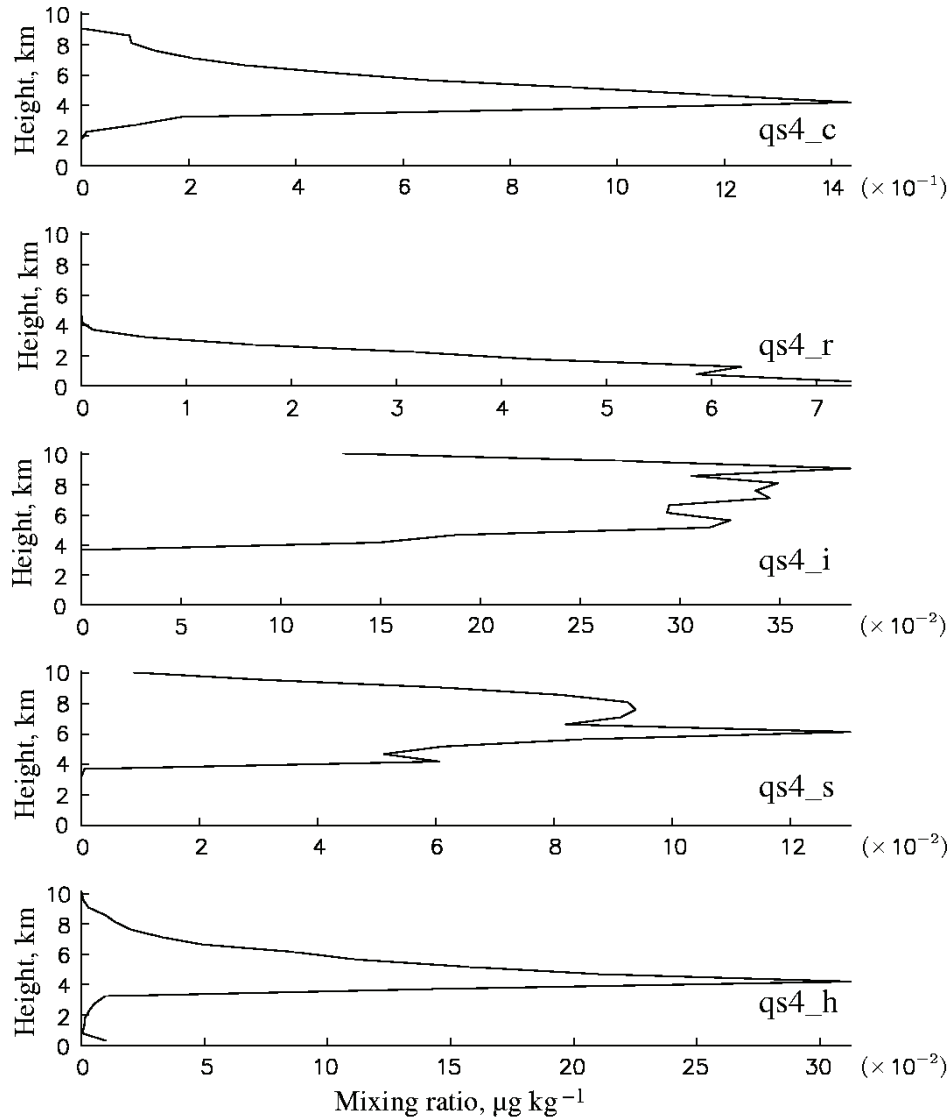It is interesting to compare the sulfate profiles in areas with different CRRs. To do this, the sulfate profile at point D (75, 75 km), which is located on the periphery of the cloud and had a CRR of 20 dBz (Fig. 7), is drawn. If this profile is compared with the previous ones, small differences in the shape of the profiles could be seen, especially for sulfate in rainwater. Specifically, at point D the

maximum value of the sulfate-mixing ratio in rainwater was not at the surface but at a height of 2 km. This is because in this part of the cloud, there was no precipitation at the surface. The most considerable differences existed in the values of mixing ratios: all sulfate mixing ratios had smaller values at point D, compared to points A, B and C. This is understandable, given that vortex D has the lowest CRR.
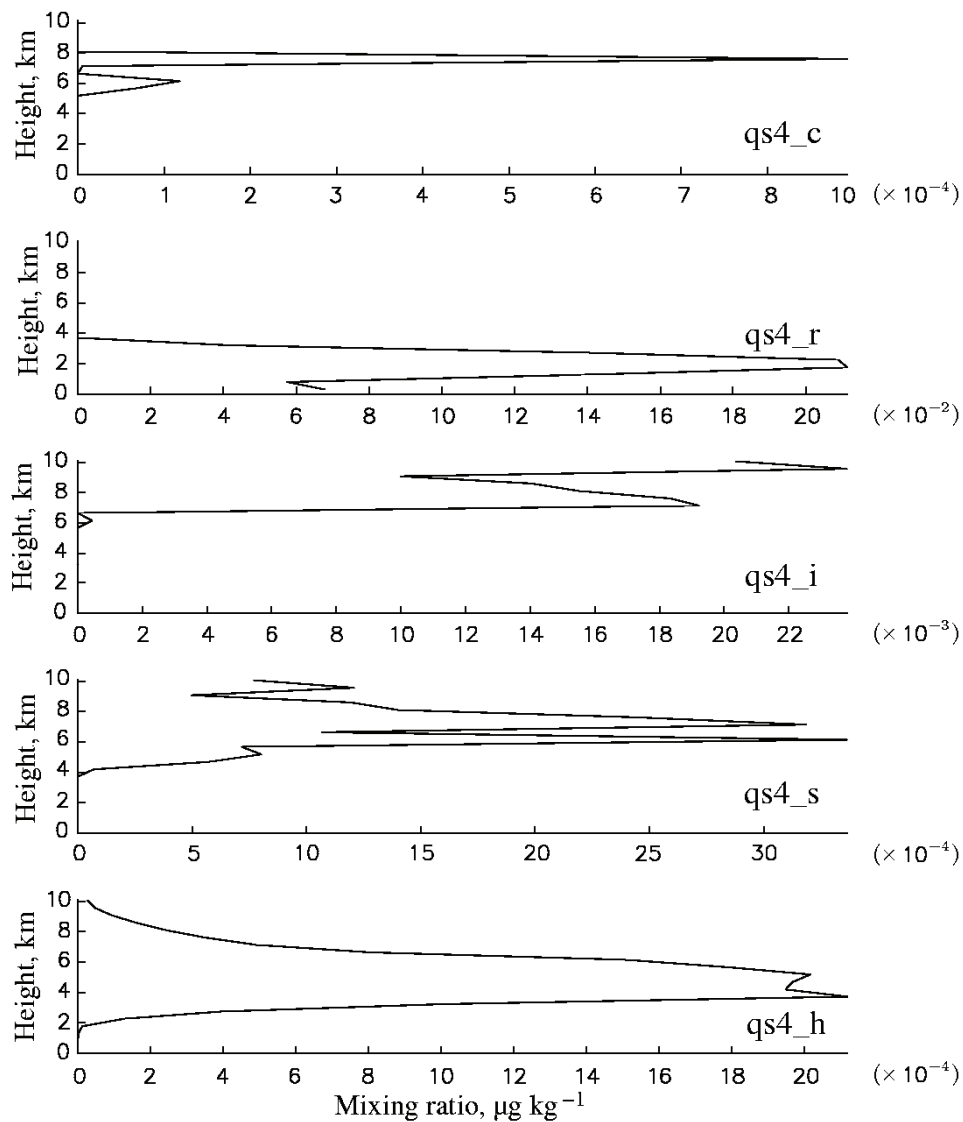

Fig. 7. The vertical profiles of the SO_4^{2-} mixing ratio, $\mu g\ kg^{-1}$, in different water categories: in cloud water ($q_{s4,c}$), rain ($q_{s4,r}$), cloud ice ($q_{s4,i}$), snow ($q_{s4,s}$) and hail ($q_{s4,h}$) at point D (75 km, 75 km) at the cloud periphery.

CONCLUSIONS

This paper described in detail the development of a chemistry module that was incorporated into a very comprehensive, mesoscale cloud-resolving model. The chemistry module contained five chemical species: SO_2, H_2O_2, O_3, SO_4^{2-} and NH_4^+. There were six prognostic continuity equations for mixing ratios of each chemical species, for each of the water categories. Two different approaches were used to express the amount of the chemical species in cloud or rainwater: the Henry Law and a fully kinetic calculation of a gas uptake. After dissolution, the chemical species were transferred from one water category to another by microphysical reactions. Oxidation of S(IV) by H_2O_2 and O_3 in cloud droplets and raindrops were included in the module due to their great importance in sulfate production processes. The pH values for cloud droplets and raindrops were calculated in every time step.

After comparing the mass of wet deposited sulfur with the results of other studies (verification), it was accepted that the model could be used as a good prognostic tool for determining the redistribution of chemical species. In this sense, the results showed that there was no loss of total sulfate mass, that the sulfate values in all water categories depended on the calculated radar reflectivity and that convective clouds provide a suitable environment for sulfate transport from the boundary layer to the upper troposphere.

SUPPLEMENTARY MATERIAL

Calculation details for the parameters *PS*1–*PS*26 are available electronically from http://www.shd.org.rs/JSCS/, or from the corresponding author on request.

И З В О Д

ХЕМИЈСКИ МОДУЛ ЗА ТРОДИМЕНЗИОНИ МОДЕЛ ОБЛАКА: ПРЕРАСПОДЕЛА СУЛФАТА

ДРАГАНА ВУЈОВИЋ и ВЛАДАН ВУЧКОВИЋ

Универзитет у Београду, Физички факултет, Институт за метеорологију, Добрачина 16, Београд

Дефинисан је хемијски модул и укључен у комплексни тродимензиони модел облака ARPS да би се испитала редистрибуција сулфата у облаку. У модел је укључена комплексна орографија Србије. У модул су укључени сумпор-диоксид, сулфатни јон, амонијумов јон, водоник-пероксид и озон. Разматрано је шест категорија воде: водена пара, облачна вода, киша, облачни лед, снег и град. Свака хемијска врста у свакој категорији воде је представљена диференцијалном једначином континуитета масе. Овај рад даје детаљан опис хемијског модула. Показује се да модел облака са укљученим хемијским модулом може да прогнозира масу сумпора депонованог влажном депозицијом, као и прерасподелу сулфата у свим категоријама воде. Главне микрофизичке и хемијске брзине конверзије сулфата осредњене на 2 h (што је период интеграције) су оксидација S(IV) у облачној и кишној води, испирање сулфата Брауновском дифузијом у облачним кап-

љицама и облачном леду и испирање сулфата кишом. Израчунате вредности сулфата у свим категоријама воде и облик профила сулфата зависе од радарске рефлексивности.

REFERENCES

1. C. G. Warren, C. J. Hahn, J. London, R. M. Chervin, R. L. Jenne, *Global distribution of total cloud cover and cloud type amounts over land*, Tech. Rep. NCAR Technical note TN-273+STR, National Center for Atmospheric Research, Boulder, CO, 1986
2. J. Hales, *Atmos. Environ.* **16** (1982) 1775
3. G. R. Taylor, *J. Atmos. Sci.* **46** (1989) 1991
4. A. Tremblay, H. Leighton, *J. Climate Appl. Meteor.* **25** (1986) 652
5. M. Niewiadomski, *Atmos. Environ.* **23** (1989) 477
6. W. C. Skamarock, J. G. Powers, M. Barth, J. E. Dye, T. Matejka, D. Bartels, K. Baumann, J. Stith, D. D. Parrish, G. Hubler, *J. Geophys. Res.* **105** (2000) 19973
7. Y. Yin, D. J. Parker, K. S. Carslaw, *Atmos. Chem. Phys.* **1** (2001) 19
8. M. C. Barth, A. L. Stuart, W. C. Skamarock, *J. Geophys. Res.* **106** (2001) 12381
9. V. Spiridonov, M. Ćurić, *J. Atmos. Sci.* **62** (2005) 2118
10. M. Xue, K. K. Droegemeier, V. Wong, *Meteor. Atmos. Phys.* **75** (2000) 161
11. M. Xue, K. K. Droegemeier, V. Wong, A. Shapiro, K. Brewster, F. Carr, D. Weber, Y. Liu, D. H. Wang, *Meteor. Atmos. Phys.* **76** (2001) 134
12. M. Ćurić, D. Janc, D. Vujović, V. Vučković, *Meteorol. Atmos. Phys.* **84** (2003) 171
13. M. Ćurić, D. Janc, D. Vujović, V. Vučković, *Atmos. Res.* **66** (2003) 123
14. Y. L. Lin, R. D., Farley, H. D. Orville, *J. Appl. Meteor.* **22** (1983) 1065.
15. J. S. Marshall, W. M. Palmer, *J. Meteor.* **5** (1948) 165
16. S. A. Rutledge, D. A. Hegg, P. V. Hobbs, *J. Geophys. Res.* **91** (1986) 14385
17. V. Spiridonov, M. Ćurić, *Idojaras* **107** (2003) 58
18. M. C. Barth, *Atmos. Res.* **82** (2006) 309
19. C. J. Walcek, H. R. Pruppacher, *J. Atmos. Chem.* **1** (1984) 307
20. S. Pandis, J. H. Seinfeld, *J. Geophys. Res.* **94** (1989) 1105
21. D. J. Jacob, *J. Geophys. Res.* **24** (1996) 113
22. C. Wang, P. J. Crutzen, *J. Geophys. Res.* **100** (1995) 11357
23. J. H. Seinfeld, S. Pandis, *Atmospheric chemistry and physics: From air pollution to climate change*, Wiley, New York, USA, 1998, p. 1225
24. H. R. Pruppacher, J. D., Klett, *Microphysics of Clouds and Precipitation*, Kluwer, Dordrecht, Germany, 2004, p. 954
25. J. Y. Liu and H. D. Orville, *J. Atmos. Sci.* **26** (1969) 1283
26. N. Molder. H. Hass, H. J. Jacobs, R. Laube, A. Ebel, *J. Appl. Meteor.* **33** (1994) 696.